UCID- 17864

Lawrence Livermore Laboratory

A STUDY OF EUV EMISSIONS FROM 2XIIB

R.P. Drake, K.I. Chen, H.W. Moos, J.L. Terry
The Johns Hopkins University
and
R.S. Hornady
Lawrence Livermore Laboratory

June 27, 1978

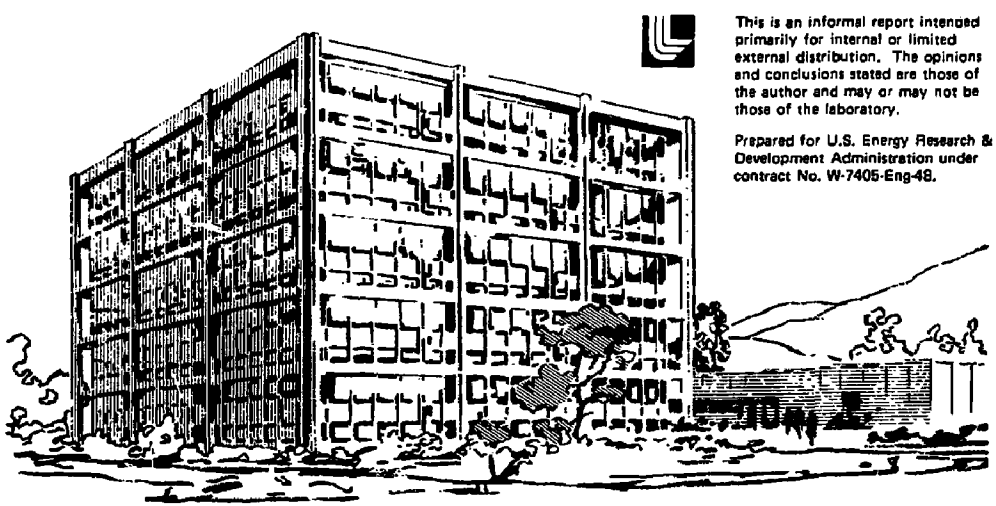

Prepared for U.S. Energy Research & Development Administration under contract No. W-7405-Eng-48.

A STUDY OF EUV EMISSIONS FROM 2XIIB*

R.P. Drake, K.I. Chen, H.W. Moos, J.L. Terry

The Johns Hopkins University

R.S. Hornady

Lawrence Livermore Laboratory

ABSTRACT

Initial results from a study of EUV emissions from the 2XIIB experiment are reported. Time-dependent brightness measurements of deuterium, oxygen, nitrogen, carbon and titanium emissions from the central 2XIIB plasma have been made. The deuterium Lyman alpha brightness is 1.5 X 10^{17} photons $sec^{-1}cm^{-2}sr^{-1}$. The Lyman alpha time development and broad spectral profile are consistent with other knowledge of the 2XIIB plasma. Oxygen is the dominant impurity in 2XIIB. The O VI 1032 Å brightness is 1.65 X 10^{18} photons $sec^{-1}cm^{-2}sr^{-1}$. The oxygen concentration is 2 % and its estimated confinement lifetime is 300 μs; this may imply mirror confinement of the oxygen ions. Nitrogen and carbon concentrations are 0.4 % and 0.3 %, respectively. It is not certain whether these impurities are mirror confined. The titanium concentration is believed to be low compared to that of oxygen. The power loss from the central plasma due to radiation by and ionization of light impurities is ∿60 kW, which is 4 % of the power deposited by the neutral beams. Further studies of impurity sources and penetration are now being performed.

*Performed under the auspices of the U.S. Department of Energy by the Lawrence Livermore Laboratory under contract number W-7405-ENG-48 and by the Johns Hopkins University under contract number EY76-S-02-2711.

Table of Contents

A STUDY OF EUV EMISSIONS FROM 2XIIB

I. INTRODUCTION

This report describes an extreme ultraviolet (EUV) spectroscopic study of impurities in the neutral beam heated mirror machine, 2XIIB. As in all high temperature plasma devices, issues such as impurity power loss and the effects of impurities on the T_e profile are of concern. On the one hand, mirror machines in particular are not expected to have an impurity problem, as they are open-ended. High Z impurities scatter into the loss cone faster than deuterium ions do. In addition, the ambipolar plasma potential should preferentially eject impurities, and should prevent their penetration from the ends. On the other hand, the success of stream stabilization of 2XIIB[1] raises questions about the effectiveness of the ambipolar potential in excluding particles, including impurities, from the plasma. In addition, impurities in the high energy neutral beams may be injected and confined despite the plasma potential. Furthermore, impurities may play a beneficial role, by means of the "Ohkawa Current",[2] in field reversal experiments. This occurs because electron currents may cancel the ion currents which reverse the magnetic field, but impurities can impede the electron currents by increasing Z_{eff}.

In view of the above considerations, a study of impurities in a machine of this type is of interest. In cooperation with the Lawrence Livermore Laboratory, the Johns Hopkins University is investigating the nature and implications of EUV emissions from the central 2XIIB plasma. The time-dependent emissions from the dominant species D, light impurities (O, C, and N) and titanium are being measured with high photometric accuracy. Data of this type can be used to address questions such as impurity

concentrations, confinement, lifetimes, sources, transport, and power loss. This report is a presentation of the initial results of that experiment. obtained during a study of the 2XIIB EUV emissions, conducted from September 19 to December 22, 1977. Some knowledge gained in early 1978 is used to interpret the data.

At the outset of this study, a surprising result was that the EUV emissions from 2XIIB are very bright, even in comparison with tokamak emissions. The oxygen concentration is large and emits substantial quantities of radiation from highly ionized states. The high power loss, due to radiation and ionization, is more than 10 W cm^{-3}. Although this power loss is a low percentage of the deposited neutral beam power, it may have implications for the larger, less intensely heated mirror experiments of the future. These and other results from this initial study are covered in this report.

The quantities presented and evaluated in this report are defined and discussed in Section II. Section III of this report is a brief description of experimental details, including the JHU spectrometer and 2XIIB parameters. Section IV reports the impurity measurements. The identified species and the measured brightnesses are presented. The time histories of impurity emissions are described, and the machine conditions for this data are discussed. Section V considers the question of power loss due to impurities, and Section VI presents the estimates of impurity confinement times, concentrations, and currents which may be obtained from the data. Section VII relates the brightness and spectral profile of the dueterium Lyman alpha emissions to the velocity distribution of the mirror confined ions and atoms from the neutral beam and surrounding gas. A summary and conclusions are presented in Section VIII.

II. BASIC CONCEPTS OF EUV DIAGNOSTICS

This section discusses the relationship of the impurity concentrations, fluxes, and confinement times to the measured EUV brightness. Note that these relationships, which are used in Section VI to compute these quantities from the empirical brightness data, are model dependent; the reliability and details of these models are improving with continued study of 2XIIB.

A. Brightnesses

The measured brightness of an emission line from an optically thin source, is given by

$$B = \frac{1}{4\pi}\int E(\underline{r})\,dl \text{ photons sec}^{-1}\text{ cm}^{-2}\text{ sr}^{-1}, \qquad (1)$$

where $E(\underline{r})$ is the volume emission rate in photons sec^{-1} cm^{-3} into 4π steradians and the integral is taken along the line of sight of the measuring instrument. $E(\underline{r})$ can be replaced by more microscopic quantities if one considers the cause of the photon emissions. The only important processes related to emission, in this type of plasma, are collisional excitation and radiative decay.* As radiative decay is much faster than collisional excitation, the emission rate is determined by the excitation rate, thus

$$E = n_e N G \langle \sigma v \rangle^{ex} \qquad (2)$$

---

*Photon excitation is unimportant as 2XIIB plasmas are optically thin; collisional de-excitation is not significant because radiative decay is much faster.

$\langle \sigma v \rangle^{ex}$ is the rate coefficient for electron impact excitation,* G is the branching ratio for the transition being measured (G = 1 for resonance transitions), N is the density of ions in the lower state of the transition, and n_e is the electron density.

One can now obtain a relationship between the measured monochromatic surface brightness of the plasma and the microscopic electron and impurity ion densities. The substition of (2) into (1) yields

$$B = \frac{1}{4\pi} \int n_e \; N\langle \sigma v \rangle^{ex} \; dl \qquad (3)$$

The transitions observed have energies on the order of 15 eV. In such cases, $\langle \sigma v \rangle^{ex}$ varies slowly with T_e above 20 eV. In consequence, $\langle \sigma v \rangle^{ex}$ can usually be withdrawn from the integral in this study. The best available excitation rate coefficients were used[3-7] to obtain the impurity concentrations.**

B. Lifetimes and Rates

The rate, ν, and lifetime τ, are defined by

$$\nu = \frac{1}{\tau} = \frac{1}{x} \frac{dx}{dt} \quad ; \qquad (4)$$

if τ is not a function of x, it is the time for exponential growth and decay of the quantity x. For collisional excitation, as described above, $\nu = n_e \langle \sigma v \rangle^{ex}$ and is typically $10^6 sec^{-1}$. For radiative decay ν is the radiative spontaneous emission rate, on the order of $10^9 sec^{-1}$ for the transitions measured here. These rates provide clear justification for the model of Eq. (3).

---

*Ion impact excitation is small compared to the uncertainty in $\langle \sigma v \rangle$, as long as the ion velocity is not comparable to the electron velocity.

**Refs. 3-7 generally agree quite well on these values. In cases of disagreement, the close coupling calculations of Robb (3) were used.

A number of atomic collision processes must be considered to understand the behavior of impurities in a plasma. Lifetimes for several processes, computed using 2XIIB parameters, are given in Table II-1 for the important ionization states of oxygen. Table II-2 presents the formulas and references used to compute these lifetimes.[4,8-13] Electron impact ionization is very fast for oxygen ions of low charge in the central 2XIIB plasma, but is less rapid for highly charged ions. Charge exchange processes,

$$O^Z + D^0 \rightarrow O^{Z-1} + D^+,$$

are important in this plasma because of the relatively large density of high energy neutrals. Charge exchange ultimately limits the population of high ionization states. In contrast, the low electron density of this plasma implies that recombination is negligible. The Spitzer drag and 90^0 scattering times given in Table II-1 imply that a high energy impurity may be confined for a few hundred microseconds, while a low energy impurity should not be confined at all. Additional processes which are still under investigation, such as deuteron impact ionization, may also affect the behavior of impurities in 2XIIB. Such processes will not be considered here.

One of the goals of this study was determination of the confinement lifetime of impurity ions in the 2XIIB plasma. The best way to determine the lifetime of observed impurities is with an accurate computer model of the plasma, including transport and using good rate coefficients. As a next approximation, a zero dimensional code can simulate transport by the use of confinement times. By successfully modeling the time behavior of impurity emissions, using known $T_e(\underline{r},t)$

TABLE II-1
Impurity Time Scales*

PROCESS	LIFETIME OF STATE FOR PROCESS IN MICROSECONDS							REF.
	OI	OII	OIII	OIV	OV	OVI	OVII	
Ionization**	0.24	0.84	2.4	6.4	22	77	3.3×10^5	(8)
Charge Exchange	0.29	270	910	33	40	50	63	(9,10,11)
Spitzer Drag		6700	1700	750	420	270	190	(12)
Recombination		1.7×10^6	8×10^4	2×10^4	4×10^4	2.5×10^6	1.2×10^6	(4)
Self-scattering Lifetime: 100 eV Oxygen		1900	120	24	7.8	3.0	1.5	(13)
10 keV Oxygen		1.9×10^6	1.2×10^5	2.4×10^4	7.8×10^3	3.0×10^3	1.5×10^3	
Oxygen off Deuterium Scattering Lifetime: 100 eV Oxygen		1100	260	120	69	45	30	
10 keV Oxygen		1.1×10^5	2.8×10^4	1.2×10^4	6.9×10^3	4.5×10^3	3×10^3	

*The following parameters are assumed
T_e = 100 eV, $n_e = 5 \times 10^{13} cm^{-3}$, $n_{D^0} = 5 \times 10^{10} cm^{-3}$, $v_{D+} = 10^8 cm\ sec^{-1}$, $n_o = 10^{12}$
**For comparison, excitation times for strong lines are typically 1 us.
(8) - Lotz, (9) - Gardner, (10) - Crandall, (11) - ORNL, (12) - Spitzer, (4) - Mattioli, (13) - Futch et al.

TABLE II-2

PROCESS	FORMULA FOR LIFETIME	REFERENCE
IONIZATION	$\tau = \frac{1}{n_e \langle \sigma v \rangle^{ion}}$	Lotz[8]
CHARGE EXCHANGE	$\tau = \frac{1}{n_o \langle \sigma v \rangle^{cx}}$ (ions) $= \frac{1}{n_e \langle \sigma v \rangle^{cx}}$ (neutrals)	Gardner[9] Crandall[10] ORNL[11]
SPITZER DRAG	$\tau = \frac{10^{13} M T_e^{3/2}(keV)}{n_e \ln \Lambda Z^2}$	Spitzer[12]
RECOMBINATION	$\tau = \frac{1}{n_e \langle \sigma v \rangle^{REC}}$	Mattioli[4]
SCATTERING	$n_b \tau_{ab} = 5 \times 10^{10} E_a E_b^{\frac{1}{2}} A_a A_b^{-\frac{1}{2}} Z_a^{-2} Z_b^{-2} \log_{10} R_m$	Futch et al.[13]

This is scattering of species a off species b neglecting potential effects, with E in keV and A in AMU.

and $n_e(\underline{r},t)$ profiles, one can in principle obtain the impurity confinement times. Unfortunately, the rate coefficients and T_e profiles needed are not precisely known. This is particularly true for charge exchange processes. In addition, consideration of the effects of impurity transport leads to both complexity and uncertainty in the model. Despite these problems, one can easily make a factor-of-two estimate of the impurity lifetime by crude methods.

Two methods of estimating impurity confinement times will be presented. First, if one knows the volume rate of influx, C (cm^{-3} sec^{-1}), of an impurity species such as oxygen, and the density of that species, then in steady state the average lifetime of that species is

$$\tau_c = \frac{N}{C} \quad , \tag{5}$$

where $N = \sum N_i$; the sum is over all ionization states. C may be found by evaluating the volume rate at which impurity ions pass through some low ionization state in which, due to its rapid ionization, confinement losses are expected to be small. The significant processes resulting in the net upward flow of impurity ions into higher ionization states are ionization and charge exchange. Thus,

$$C = N_i n_e \langle \sigma v \rangle_i^{ion} - N_{i+1}\, n_o \langle \sigma v \rangle_{i+1}^{cx} \tag{6}$$

The volume rate of ionization is $N_i n_e \langle \sigma v \rangle_i^{ionization}$; N_i is the density of impurities in the low ionization state determined from the EUV data, and $\langle \sigma v \rangle_i^{ion}$ is the rate coefficient for electron impact ionization out of state i. The volume rate of charge exchange, is $N_{i+1} n_o \langle \sigma v \rangle_{i+1}^{cx}$; n_o is the neutral deuterium density and $\langle \sigma v \rangle_{i+1}^{cx}$ is the rate coefficient for charge exchange into state i.

The second method of estimating impurity lifetimes is simpler than the first. An impurity species must in general be confined long enough to reach the ionization state observed to be most populous. This time is the sum of the ionization times for each state below the most populous state, Z:

$$\tau_c = \sum_{i<Z} \tau_i = \sum_{i<Z} \frac{1}{n_e \langle \sigma v \rangle_i^{ion}} \qquad (7)$$

This value is a minimum estimate of the confinement time because it does not include the impurity lifetime in the most populous ionization state. τ may be significantly underestimated if the impurity confinement time in the terminal states is long compared to the ionization times considered.

C. Impurity Densities and Concentrations

If one knows $n_e(r)$, $T_e(r)$ and the spatial profile of the impurity ions, then Eq. (3) can be integrated to obtain the impurity density of that ionization state. If this can be done for all ionization states of a given impurity species, the total density of that species and hence its concentration in the plasma are known.

As a practical matter, one does not know the impurity spatial profiles very well, so one uses simple models, three of which will be mentioned here: the flat profile, the Gaussian profile, and the thin shell model. If the impurities are evenly distributed, and the T_e profile is sufficiently broad, both n and $\langle \sigma v \rangle^{ex}$ can be removed from the integral in (3), yielding

$$N_i = \frac{4\pi B}{\langle \sigma v \rangle^{ex} \int n_e dl} \ (cm^{-3}) \qquad (8)$$

(Spatial scans conducted in early 1978 and Thomson scattering data indicate that this is the appropriate model for 2XIIB.) In the second model, the n_e and n profiles are both approximately Gaussian (and $\langle \sigma v \rangle^{ex}$ = const.) and Eq. (3) can be integrated directly. Finally, if the impurity ions exist

in a shell at r = a, Eq. (3) becomes

$$B = \frac{1}{4\pi} n_e(a)\, n \langle \sigma v \rangle^{ex}\, 2\Delta w, \tag{9}$$

where Δw is the shell thickness.

D. Impurity Currents and Fluxes

The total number of impurities per second entering the plasma is the impurity current. This current, expressed in equivalent amperes, is

$$I = e \int \frac{N}{\tau} \, dV \ . \tag{10}$$

The impurity current is useful for comparison with known sources of deuterium. The current calculated in this report is that entering the central plasma, given by

$$I = \frac{eNV}{\tau_c} = \frac{eN\pi R_p^2 L}{\tau_c} \ . \tag{11}$$

The value of N used in Eq. (11) should be consistent with the densities and population distributions involved in the estimation of τ_c by Eq. (5) or Eq. (7). The relation of the current to the average impurity flux is

$$\Gamma = \frac{I}{A} \ . \tag{12}$$

A is the area over which the impurity current enters the plasma. A good discussion of impurity fluxes and their estimation is presented in Ref. 14.

The impurity flux may be directly estimated for inward moving impurities which form concentric shells of increasing ionization state as the radius decreases and the temperature increases in a sheath. If the impurities ionize faster than they diffuse or charge exchange, the flux at the radius

is[14]

$$\Gamma = 2\pi B \frac{\langle \sigma v \rangle^{\text{ionization}}}{\langle \sigma v \rangle^{ex}} \qquad (13)$$

Eq. (13) may be seen to represent the impurity flux as the photon flux ($4\pi B$) divided by the average number of photons emitted per ion ($\langle \sigma v \rangle^{ex} / \langle \sigma v \rangle^{ion}$) for a shell observed twice along the line of sight. If the impurities enter the plasma by another means, such as neutral beam injection, Eq. (13) does not apply. However, the implication of Eq. II-(8), (11), and (12) is that a high value of the brightness implies a high concentration, and hence a large impurity flux or/and a long confinement time.

III. EXPERIMENTAL DETAILS

The JHU spectrometer has been described in detail elsewhere,[15] as has the 2XIIB plasma device.[16] This section contains a brief description of the spectrometer, the plasma device and the experimental setup at 2XIIB. The orientation of the spectrometer is shown in Fig. III-1. Figure III-2 exhibits data indicating some of the 2XIIB plasma characteristics.

A. Spectrometer System

The instrument is a 0.4 m normal incidence extreme ultraviolet monochromator. It utilizes a 2400 line/mm platinum coated grating blazed at 300 Å, and a windowless photomultiplier tube with a Cu I photosensitive surface to obtain a spectral range of 300 Å to 1700 Å; the time resolution is 70 microseconds. Typical slit settings were 2 Å (FWHM) to completely cover the spectral line width.

The instrument has been absolutely calibrated at the National Bureau of Standards (on the SURF-II synchrotron radiation source) and at JHU using NBS diode detectors as the calibration reference.[17] These calibrations agree. The estimated total uncertainty in the absolute sensitivities was

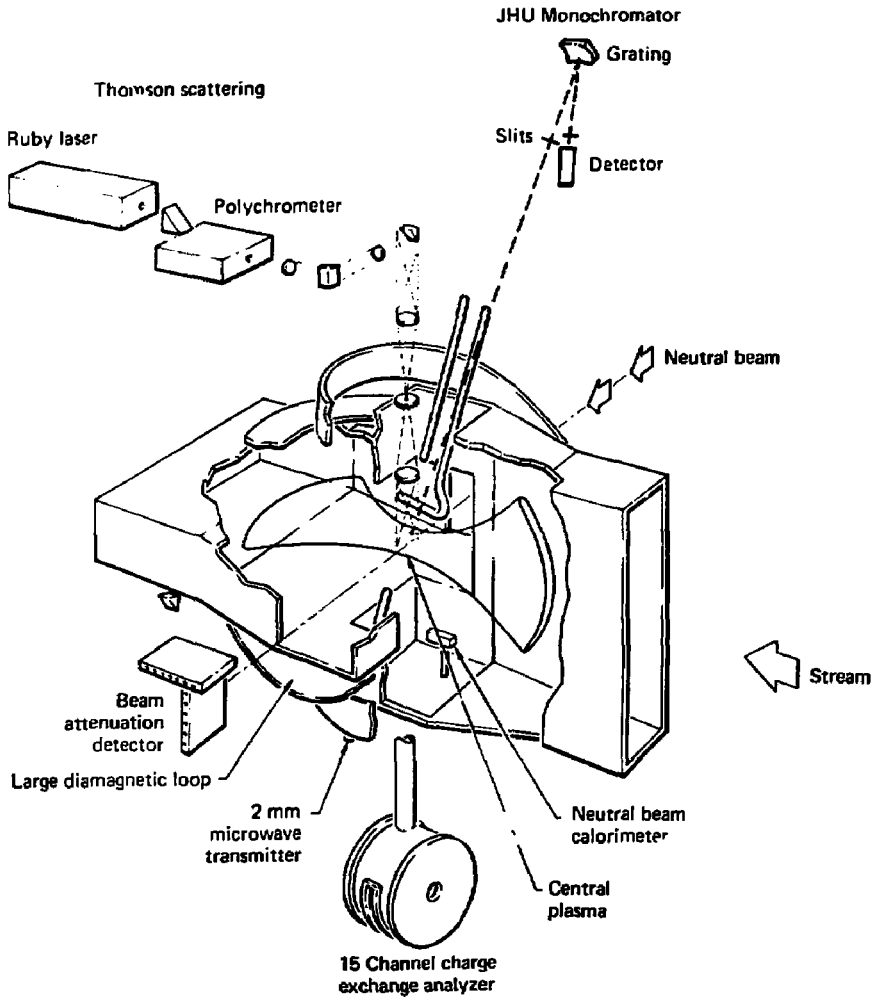

Figure III-1. Schematic of selected 2XIIB diagnostics, including EUV monochrometer system.

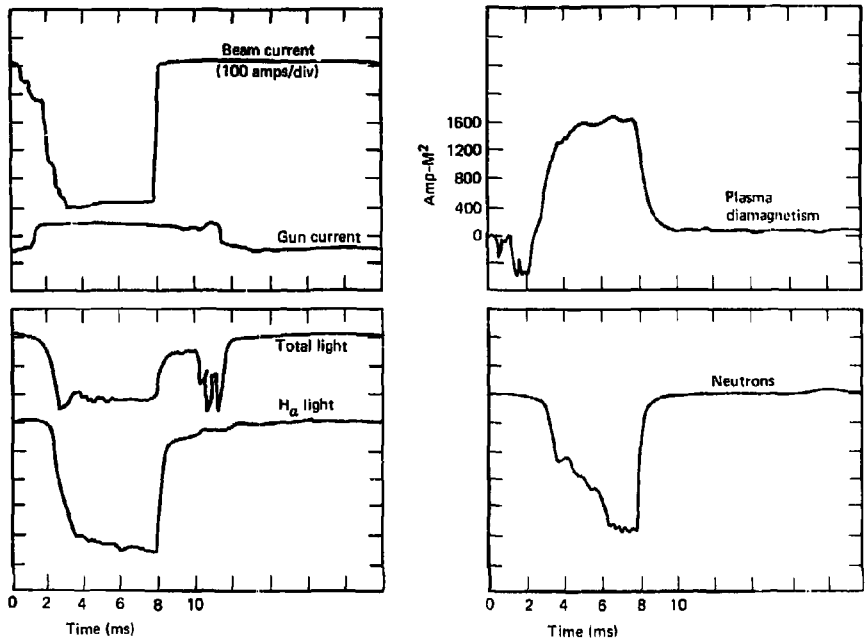

Figure II-2. 2XIIB diagnostic traces from shot 25 Oct. 24, 1977.

less than ±25%. This value is subject to drifts in the calibration, which will be determined at the end of the present experiment. The monochromator is equipped with a preslit, 40 cm from and parallel to the entrance slit, which allows selective variation of the width and center of the field of view; an MgF_2 window enables elimination of second order radiation above 1150 Å.

Some special preparations were made for the 2XIIB experiment. The spectrometer slits were recalibrated, and the absolute sensitivity calibration was repeated. New magnetic shielding was designed, constructed, and tested to protect the photomultiplier from the 500 gauss fields near 2XIIB.

B. 2XIIB Parameters and the Spectrometer Installation

2XIIB is a neutral beam heated minimum-B geometry plasma confinement device.[16] For the oxygen results obtained October 24, which are emphasized in this report, it produced high beta (beta > 1) plasmas in a 6.7 kG central vacuum field. The electron temperature was typically 150 eV; the ion temperature was approximately 13 keV. Line densities were about 1.5 X $10^{15} cm^{-2}$, with a 7 to 10 cm radius and a Gaussian radial profile implying a peak density of 1 X $10^{14} cm^{-3}$. The hot plasma had a 15 to 18 cm 1/e axial halfwidth.

The JHU instrument is positioned on top of 2XIIB and looks down through the yin yang coils into the midplane region. The entrance slit is 2.8 m from the machine center, about 13 degrees north and 3 degrees east of the vertical axis. The line-of-sight is through the hot plasma in the center of 2XIIB (See Fig. II-1). The field of view is typically 1 cm radially by 3 cm along the magnetic axis. The spatial alignment of the spectrometer was tested by scanning the plasma, and was found to be approximately correct.

IV. EUV EMISSION CHARACTERISTICS

The basic experimental data, which will be further analyzed later, are presented in this section. The observed impurity ions are listed; also described are the time development and absolute brightnesses of the impurity emissions. Brightness measurements of both the target plasma formed by washer stack guns and the hot plasma established by neutral beam injection are reported, as well as the machine conditions during these experiments. A brief discussion of the washer guns as an impurity source is given in subsection D.

A. Observed Ions and Emission Characteristics

Spectral emission lines due to ionization states of oxygen, nitrogen, carbon, and titanium have been observed. The lines observed are tabulated in Table IV-1, which includes an indication of our confidence in their identification. This confidence level is based on observation of the transitions from another plasma with the same instrument, and our ability to scan the spectral region, given a limited number of shots at constant machine parameters. The observed transitions are indicated; they are all ground state resonance transitions. Typical time histories of five oxygen states are presented in Figs. IV-1 and IV-2.

The time deveopment of the 2XIIB discharge can be divided into three phases: The target plasma buildup, the hot plasma buildup, and the high density plateau. During these experiments, a target plasma was provided by titanium washer guns beginning at 1.2 ms after machine "zero time". The hot plasma buildup began when the neutral beams fired at 1.8 ms and ended when the high density plateau was reached at about 4 ms. The plateau lasted until about 8 ms, depending on the duration of the neutral beam current.

During the target plasma buildup, low intensity impurity emissions were observed from low ionization states. Emissions of O II and O III were

TABLE IV-1

Observed Ions and Transitions

Ion	λ(A)	Transition		Confidence
HI	1216(L_α)	1s - 2p	$^2S - ^2P$	A
O VI	1032	2s - 2p	$^2S - ^2P$	A
O V	630	$2s^2$-2s2p	$^1S - ^1P$	A
O IV	554	$2s^22p$-2s$2p^2$	$^2P - ^2P$	A
O III	703	$2s^22p^2$-2s$2p^3$	$^3P - ^3P$	A
O II	539	$2p^3$-$2p^2$3s	$^4S - ^4P$	A
C IV	1548	2s - 2p	$^2S - ^2P$	A
C III	977	$2s^2$-2s2p	$^1S - ^1P$	A
N V	1239	2s - 2p	$^2S - ^2P$	A
N III	685	$2s^22p$-2s$2p^2$	$^2P - ^2P$	A
Ti VII	522	$3s^23p^4$-3s$3p^5$	$^3P - ^3P$	C
Ti IV	779	3d - 4p	$^2D - ^2P$	B

All transitions are ground state resonance transitions.

Confidence Key:
A-GOOD Observed and scanned here and elsewhere with this equipment.
B-GOOD Observed and scanned in this study only.
C-POOR Incompletely scanned in this study only.

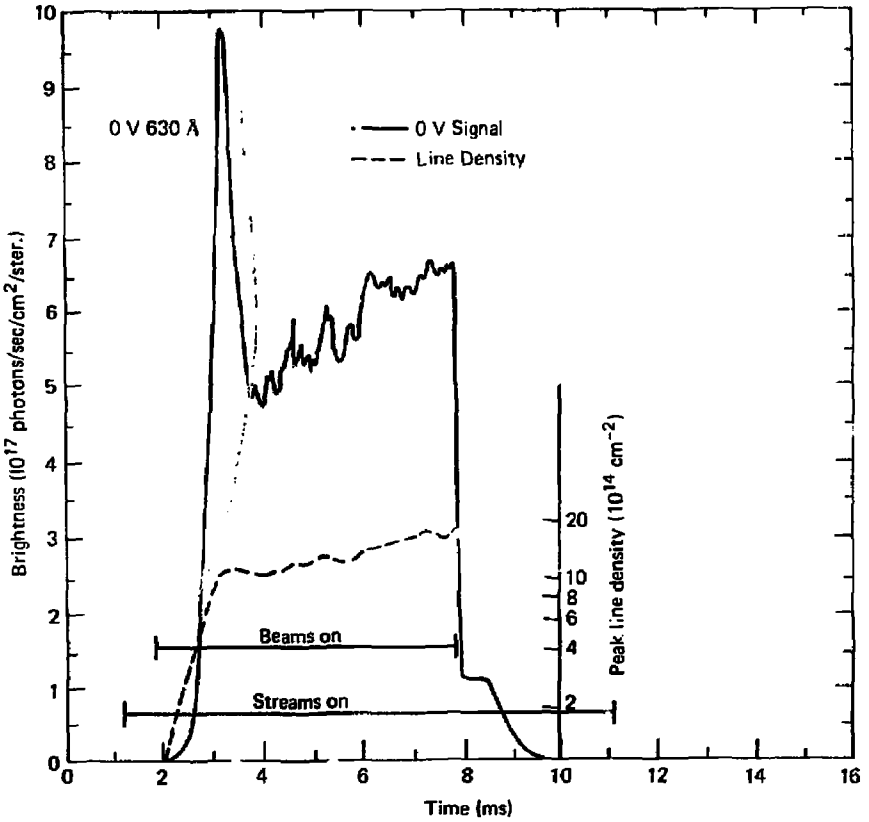

Shot 25 10/24/77

Parameters at 6 ms

T_e	175 eV
E_i	13 KeV
Radius	9.5 cm
Line Density	1.5 X 10^{15} cm^{-2}
Magnetic Moment	1600 Amp-m^2
Neutral Beam Current	510 Amps
Mirror Ratio	2

Figure IV-1. A typical 0 V time history, including early emission peak. Some plasma parameters and beam and stream durations are also shown. The dotted line is the line density time history.

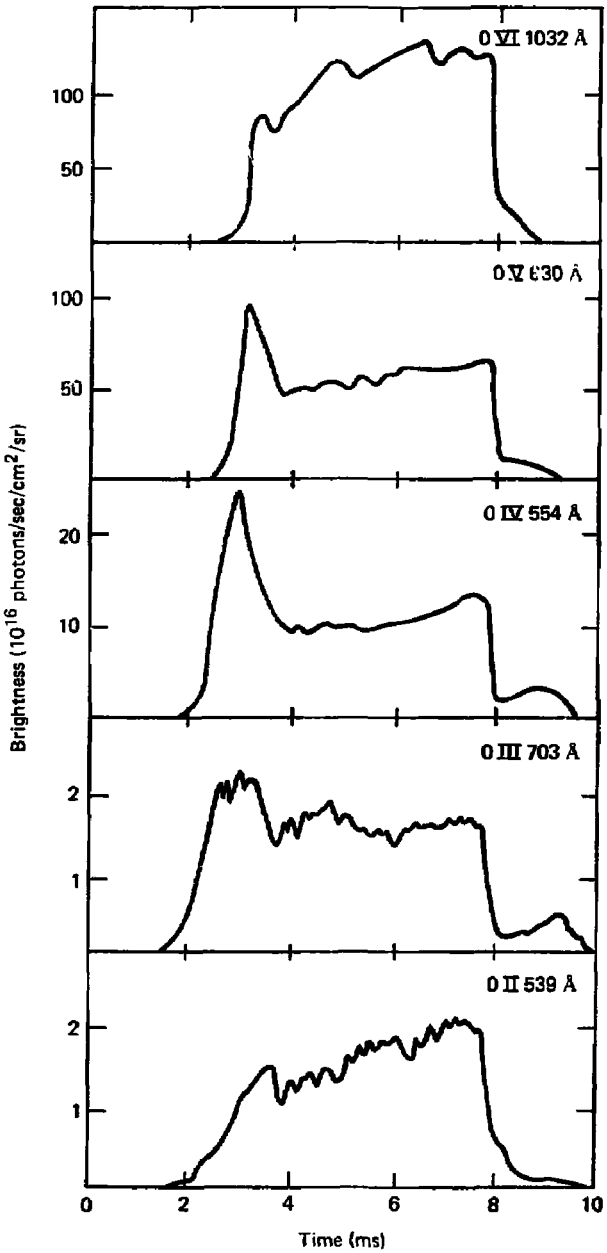

Figure IV-2. Typical emissions of the observed oxygen ions, from a series of identical shots on October 24, 1977.

observed by 1.4 ms, and O IV was observed by 1.8 ms. The emissions at this time were so dim as to require measurement on a more sensitive scale than that shown in Figure IV-2.

A strong increase in EUV impurity emissions occured during the hot plasma buildup. Brightness peaks were observed from O IV, O V, and sometimes O VI. These are believed to have resulted from the ionization of O II and O III ions already existing in the target plasma.

Impurity emissions showed some variations during the high density plateau. Emissions from low ionization states often increased during this period, while emissions from higher ionization states exhibited variable changes. These variations were usually less than a factor of two.

B. Absolute Brightness Measurements

The absolute brightness (photons $sec^{-1}cm^{-2}sr^{-1}$) emitted from the plasma is the quantity directly measured by the EUV instrument. A summary of the brightnesses during the high density plateau is presented in Table IV-2.

Several factors contribute to the uncertainties in these measurements. The obvious factors of calibration accuracy and shot-to-shot variation are considered. In addition, the effects of doppler broadening and background light levels are taken into account. Doppler broadened lines were observed, but were not studied in detail.

The most striking fact is that EUV radiation from 2XIIB is very bright. The OV and OVI brightnesses presented in Table IV-2 are more than two orders of magnitude larger than those reported from Alcator,[18] and an order of magnitude greater than those from TFR,[14] yet those tokomaks have more than an order of magnitude greater deuterium confinement time than 2XIIB. This indicates that the impurity fluxes or/and the confinement times are relatively high (See Section II-D).

TABLE IV-2

High Density Plateau Brightnesses

Ion	(A)	Plateau Brightness (10^{16}ph/sec/cm^2/ster)	Brightness/$\langle\sigma v\rangle^{ex}$ (10^{24}ph/cm^5/ster)
O VI	1032 line	165 ± 65	97
O V	630 line	70 ± 26	25
O IV	554 multiplet	10 ± 5	7.4
O III	703 multiplet	1.6 ± 0.9	1.6
O II	539 multiplet	1.05 ± 0.55	2.6
C IV	1548 doublet	11.6 ± 6.7	2.0
C III	977 line	1.15 ± 0.44	0.18
N V	1239 line	31.6 ± 16	14.1
N III	685 multiplet	1.2 ± 0.76	0.49
Ti IV	779 line	1.6 ± 0.75	*

Uncertainties include scatter in the data, calibration uncertainties, doppler broadening effects, and background light variations. These values apply to plasmas of Oct. 24, 1977 and to similar plasmas on other days.

*No reliable $\langle\sigma v\rangle^{ex}$ is available.

Table IV-2 also shows that oxygen is the dominant light impurity in 2XIIB. The right hand column presents the measured brightnesses divided by the rate coefficients for excitation of these transitions. This quantity is proportional to the average density of these ions. These coefficients are relatively insensitive to T_e above 20 eV, and were evaluated at 100 eV for this calculation. It is quite clear that oxygen densities are greater than equivalent ion densities of other species.*

C. Machine Conditions for These Measurements

Impurity studies can be questioned if the data analyzed is not taken during representative machine operation, or merely applies to a particluar "bad" or "good" day. Such objections do not apply to this study, as will be shown in this subsection.

The oxygen data analyzed here was taken on Oct. 24, 1977. This was a day of good machine operation; a description follows. The purpose of this run was to observe the effects of cooling the neutral beam tank liquid nitrogen liners. No major changes were observed in plasma parameters or oxygen emissions as the liners cooled. Before the end of this run, but after the liners were cold, a number of shots were used to obtain the data presented in the previous subsection. The machine was gettered before each shot in the usual manner, and the getter wires were in good condition. The plasma parameters presented in Figures III-2 and IV-1 are typical for this day, and show that this plasma was a normal one for this period.**

---

*Ti densities are believed to be low on the basis of observations of Ti VI and Ti VII during 1978.

**T_e was typically 150 eV for these shots, with $\pm$25 eV variations from shot to shot. These variations in T_e are not observed to effect EUV emissions or other plasma parameters.

In addition, the oxygen transitions reported in Tables IV-1 and IV-2 were all measured on at least one other day during October (with roughly comparable plasma parameters). In every such case the brightness was within a factor of two of that measured on October 24. Table IV-3 presents O V (630 Å) data from several days which span the period of this study. This table indicates that oxygen emissions do not vary greatly on a day-to-day time scale, and that the October 24 data is not unusual during that period.

The nitrogen and carbon data presented here were obtained on Nov. 2 and Nov. 3; the titanium data was obtained Oct. 14. These runs were not atypical, although these measurements were made with lower beam current and T_e($T_e \sim 70$ eV) than the oxygen measurements of Oct. 24. On Oct. 14 and Nov. 2 various stabilizing stream gun configurations were tried. The change in plasma parameters with a systematic variation of the neutral beam current during the Nov. 3 run showed that the plasma was similar to that studied over the preceeding six months. Carbon, nitrogen and titanium emissions had roughly comparable brightnesses on other days, although the data is not as extensive as that available for oxygen.

In summary, the oxygen data presented here was obtained under normal operating conditions, and there is no reason to suspect that the other impurity measurements are atypical.

D. Titanium Washer Gun Observations

Table IV-4 presents the approximate brightnesses observed from plasmas created by a single 1/2" diameter washer gun, operated on a 2 ms 6 to 8 kv pulse line. These plasmas are quite variable, and hence only approximate brightness values are given. In this case the carbon light is much brighter than that of oxygen or nitrogen. This suggests that carbon is the dominant

TABLE IV-3

Brightness of O V (630 Å) on Various Days

Date	Shot	Brightness ph $sec^{-1}cm^{-2}sr^{-1}$ (Plateau)	$\int n_e dl$ cm^{-2}
9/23/77	20	8.2×10^{17}	7×10^{14}
10/14/77	4	3×10^{17}	7×10^{14}
10/20/77	38	7.5×10^{17}	1.3×10^{15}
10/24/77	25	7.1×10^{17}	1.5×10^{15}
10/28/77	32	8.9×10^{17}	1.8×10^{15}
11/3/77	36	4.8×10^{17}	7×10^{14}
12/21/77	26	1.7×10^{18}	1.5×10^{15}
12/22/77	7	2×10^{18}	1.5×10^{15}

TABLE IV-4

Streaming Plasma Observations

Ion	Wave-length	Approximate Brightness
O II	539 Å	1×10^{15}
C III	977 Å	1.5×10^{16}
N III	685 Å	6×10^{14}
Ti IV	799 Å	$>2 \times 10^{15}$
D I (L_α)	1215.4 Å	5×10^{14}

impurity from these washer guns, with the possible exception of Ti.* This conclusion was also reached in a study of similar plasmas performed on 2XII.[19]

Every impurity species identified during beam-fueled discharges has been observed in washer gun plasmas. However, it is believed that the washer guns are not the only source of impurities on 2XIIB. The proportions of various impurities observed during beam-fueled discharges is quite different from those observed in the target plasma. (Compare Tables IV-2 and IV-4.) Furthermore, for oxygen, the impurity fluxes required to produce the observed O II brightnesses are much greater for beam fueled discharges than for washer gun created plasmas. Moreover, it is difficult to understand penetration of the plasma potential by quantities of cool streaming plasma impurities travelling along field lines. Further studies of 2XIIB will address the question of impurity sources in more detail.**

V. POWER LOSS DUE TO LIGHT IMPURITIES

Plasma impurities are of interest in part because they can radiate large

---

*More recent measurements suggest that titanium densities are greater than carbon densities in these plasmas. Titanium was excluded from 2XII by time-of-flight trapping.

**Pulsed air leaks are not normally an impurity source. One such leak existed on 9/23/77 and was identified and eliminated with the aid of the JHU spectrometer. Large increases in the nitrogen and oxygen signals were observed, beginning about one thermal transit time (from the vacuum chamber wall to the plasma) into the discharge. It is therefore clear that thermal gas, in sufficient quantities, can penetrate the 2XIIB plasma.

quantities of power. The absolute brightness measurements described above enable one to calculate the impurity power losses from 2XIIB. The method of calculation and the results for radiation, ionization and electron heating are presented below. The light impurity power loss is found to be about 63 kW, which is 4% of the 1.5 MW deposited by the neutral beams. This low percentage is due to the high density of energy deposition produced by neutral beam heating.

It must be emphasized that these results apply only to the light impurities (O, C and N) in the central plasma. The regions outside the central plasma contain several times as many particles, and may have a higher concentration of impurities producing a much larger radiation loss. While the effect of the impurities in the central plasma appears to be small, the total role of impurities in the 2XIIB power balance is not clear.

A. Theory of Spectroscopic Power Loss Measurements

Spectroscopy provides an indirect measurement of power loss due to line radiation. The determination of power loss from absolute brightnesses is described in this section. Bolometric measurements are a desirable check on the completeness of these calculations, but such measurements have not been made on 2XIIB.

There is no universal relation between power loss and brightness. The measurad brightness results from an integration of light emitted along a line of sight through the plasma:

$$B = \frac{1}{4\pi} \int E(r)dl. \qquad (1)$$

Power loss by contrast results from the emission of light throughout the plasma volume:

$$P_L = h\nu \int E(r)dV. \qquad (2)$$

P_L is the power radiated from the plasma by a spectral line with energy $h\nu$.

Once the spatial variation of E(r) is known one can relate power loss directly to brightness. Assuming cylindrical symmetry and a plasma of length L, one obtains

$$B = \frac{1}{2\pi} \int_0^\infty E(r)dr, \quad \text{and} \tag{3}$$

$$P_L = 2\pi h\nu L \int_0^\infty E(r)rdr. \tag{4}$$

Spatial scans of 2XII8 (from early 1978) show that the radial profile of E(r) is approximately Gaussian. Taking $E(r) = Ae^{-r^2/a^2}$ we obtain:

$$B = \frac{a}{2\sqrt{\pi}} A \quad \text{and} \tag{5}$$

$$P_L = \pi h\nu L a^2 A . \tag{6}$$

Hence

$$P_L = 2\pi^{3/2} h\nu L a B . \tag{7}$$

This gives the relation of power loss to measured brightness, assuming cylindrical symmetry and a Gaussian emission profile.

The total radiated power is desired, but Eq. (7) gives only the power radiated by an observed line. It is not practical to observe all radiating lines, so a calculation is necessary. It is necessary to relate the total power loss to the measured brightnesses. This relation is developed below.

As $\varepsilon(r)$ is proportional to $\langle\sigma v\rangle^{ex}$, the rate coeffecient for electron impact excitation of the transitions, one has:

$$P_L \alpha \frac{\langle\sigma v\rangle^{ex}_L}{\lambda_L}$$

The relation of this power to the power radiated by all lines of an ionization state, P_S, is

$$P_S = F\, P_L \text{ , where} \tag{8}$$

$$F = \left[\sum_i \frac{\lambda_L}{\lambda_i} \frac{\langle \sigma v \rangle_i^{ex}}{\langle \sigma v \rangle_L^{ex}} + R_m \sum_j \frac{\lambda_L}{\lambda_j} \frac{\langle \sigma v \rangle_j^{ex}}{\langle \sigma v \rangle_L^{ex}} \right] \tag{9}$$

The first sum is taken over the significant ground state transitions; and the second expression is summed over the important metastable transitions. The best values of $\langle \sigma v \rangle^{ex}$ exist for the transitions to the lowest excited states. The ratios of the other rate coefficients to these well known ones (i.e., $\langle \sigma v \rangle_L$) were estimated[20] using standard formulas[21] and the oscillator strengths of Wiese et al.[22] R_m is the ratio of metastable populations to ground state population. By including all relevant proportionalities, F converts the power radiated by the line into that radiated by the entire ionization state. Other ionization states may be included in F in the same way the metastable system is in Eq. (9), but this is less desirable; in this study it was only necessary in the unimportant case of N IV.

The radiated power loss due to an entire species is then given by

$$P_{SPECIES} = \sum P_S \tag{10}$$

These uncertainties in these calculations have several sources. The absolute calibration of the spectrometer, the use of the spectrometer, the model relating radiated power to brightness, and the

power factor F all contribute to the uncertainty. However, as the relative populations of various ionization states need not be considered, this method is considerably more accurate than a purely a priori computation.

B. Radiated Power Loss Results

The power loss due to impurities was calculated as described above. Brightness measurements have been made for all important ionization states of oxygen and for the significant states of carbon and nitrogen. All $\Delta n = 0$ and $\Delta n = 1$ transitions were considered in evaluating the power factor. Metastable ratios were taken from measurements performed on Alcator,[23] except for the important case of O V, which was checked in the 2XIIB plasma. The emission radius was taken to be 9 cm, and the length to be $15\sqrt{\pi}$. The results of these calculations are presented in Table V-1.

Most of the power radiated by 2XIIB impurities is from OV and OVI. This is due to the dominance of oxygen and to the fact that nitrogen and carbon reach helium-like states at lower temperatures than oxygen does.

C. Additional Impurity Power Loss

Impurities also remove power from plasma electrons by means of ionization and electron heating.[14] This power loss depends on the rate of impurity influx, the maximum ionization state the impurities reach, and the number of cold electrons they produce in the plasma. The impurity influx and ionization are considered in Section VI. On the basis of those results, the ionization and electron heating power loss are found to be 20 kW, with an upper limit of 62 kW. These losses are an appreciable fraction of the total impurity power loss, but are small compared to the input power to 2XIIB.

TABLE V-1

LIGHT IMPURITY RADIATED POWER LOSS

Species	Power Radiated by Measured Lines	Total Power Radiated by Species
OXYGEN	15.6 kW	35.5 kW
NITROGEN	1.44 kW	6.5 kW
CARBON	0.5 kW	0.6 kW
TOTAL	18 kW	43 $\pm$ 28 kW

Other more subtle processes may contribute to the impurity related power loss. For example, charge exchange processes in which deuterons gain electrons could lead to the loss of high energy particles from the plasma. These processes have not yet been considered in detail.

D. Implications of 2XIIB Power Loss

Apparently, the light impurities in the central 2XIIB plasma do not play a major role in determining its parameters. Neither T_e nor the T_e radial profile will be significantly affected by power losses such as these. The electron temperature limit due to impurity power loss may be estimated by equating this power loss to the Spitzer drag power input to the electrons from the hot ions. The power loss determined above allows a maximum 2XIIB electron temperature of about 500 eV, which is much higher than the observed values of T_e. One must conclude that if impurity radiation is a significant power loss mechanism in 2XIIB, this must be due primarily to impurities in the end fans.

However, there are broader implications of this result. The power loss from 2XIIB is about 10 W cm^{-3}. While this is small compared to the 280 W cm^{-3} deposited by the neutral beams*, it is not small in the context of mirror experiments with larger volumes and large surface areas. The TMX plasma volume is about 1.7 X 10^6 cm^{-3}.[24] A 10 W cm^{-3} power loss on TMX would imply 17 MW of impurity power loss, whereas the planned power deposition is <5 MW. On the other hand, transport effects and increases in T_e are expected to significantly decrease the power loss from the large solenoidal volume of TMX. It is

---

*For comparison, a typical tokamak might deposit 1 W cm^{-3} and radiate 0.3 W cm^{-3}.[14]

clear that impurities will become a major consideration in the design and operation of large mirror experiments.

VI. LIGHT IMPURITY RESULTS

The methods described in Section II were used to determine the concentrations and lifetimes of the light impurities in 2XIIB. Table VI-1 presents these results; they are discussed below. Table VI-1 bears out the initial conclusion of Section III that oxygen is the dominant impurity in 2XIIB. The scattering of deuterium off this oxygen and other similar plasma effects have not yet been considered.

The calculation of impurity densities involved a sum over all ionization states, using Eq. (8) of Section II. These calculations show that the 2XIIB plasma is mostly deuterium, but that it has a higher concentration of impurities than a clean tokamak.[18] These results imply that

$$Z_{eff} = \sum N_i Z_i^2 \; / \; N_i Z_i$$

is 1.85 ± 0.4 at the center of 2XIIB. The principal uncertainties in these estimated densities are the populations of unmeasured Helium-like ionization states, such as O VII. These populations were estimated by the balance of ionization into and charge-exchange out of these states.

The lifetime of oxygen was estimated by using Eq. (II-5) and calculating the volume rate of input from O IV to O V (Eq. II-6). The result was 280 μs. This is comparable to the Spitzer drag time for O VI at the center of the plasma of 10/24.77, which was 260 μs. (T_e was 150 eV and $\hat{n}_e$ was 9.4×10^{13} cm^{-3}) This suggests that the oxygen is mirror confined.

TABLE VI-1

LIGHT IMPURITIES IN 2XIIB

Species	Concentration at Plasma Center	Lifetime	Current to Central Plasma
OXYGEN	1.7% (Factor of two)	280 μs (>40μs)	10 amps (<23)
NITROGEN	0.4% (Factor of three)	50 μs (>25μs)	5 amps (<25)
CARBON	0.3% ± 0.2%	40 μs (>13 μs)	2 amps (<10)

As shown below, estimates of τ_c based on reasonable models of the 2XIIB potential imply that low energy impurities will leave the central plasma in less than 20 μs, during which time most oxygen ions should not even become O VI. It appears that the oxygen in 2XIIB is either injected with a high transverse velocity or rapidly heated to become mirror confined.

The ejection time for a cold impurity ion depends on the plasma potential. Once the cold impurity has gone a significant distance, such as 10 cm, it should not return to the midplane as it cannot climb the potential hill and is not mirror trapped. If one considers a Z = 1 oxygen ion accelerated by a 100 volt potential declining uniformly from the midplane to the mirror at 75 cm, one finds it travels 15 cm in 14 μs. A better model describes the variation in ϕ according to the Boltzmann relation and the measured plasma scale length:

$$\hat{n}_e e^{-z^2/b^2} = \hat{n}_e e^{-q\,\phi/kT} \quad .$$

Here z is the dimension along the magnetic field and b is the 1/e halfwidth of the axial plasma density profile. This way, taking the electric field

$$E = \frac{d\phi}{dz} \quad ,$$

one finds that a thermal Z = 1 impurity travels 16 cm in 20 μs. These results support the conclusion stated above.

The total oxygen entering the central plasma was computed by using Eq. (11) of Section II. This current applies to that oxygen which contributes significantly to the higher oxygen ionization states. If cold oxygen was impinging on the plasma surface and was being rapidly lost, these

measurements would not reveal it. A detailed study of O II emissions will be necessary to evaluate that possibility.

The nitrogen and carbon densities and currents were evaluated by the same techniques as those of oxygen. Limits on unobserved states (N IV,N VI, C V) were determined by considering ionization and charge exchange rates into and out of observed ionization states. The nitrogen and carbon lifetimes were computed using the simpler method of Eq. II-(7), which required less data. These estimates do not indicate whether the nitrogen and carbon are mirror confined, or both and particularly carbon are low energy and short-lived.

VII. LYMAN ALPHA MEASUREMENTS

A spectral study of the Lyman alpha deuterium line was also performed on October 25 and 28, 1977. The observed line profile is presented in Fig. VII-1, and Fig. VII-2 shows the time development of the entire line. This experiment may be considered a prototype demonstration of a Lyman alpha diagnostic to measure neutral deuterium velocity distributions. Although the two angstrom resolution used and the shot to shot variation of the 2XIIB plasma preclude the observation of fine details of the Lyman alpha spectrum, the observed profile is consistent with knowledge of the neutral deuterium in 2XIIB obtained from other diagnostics. The basic analysis of this profile is described below.

The full width at half maximum (FWHM) of the observed line profile is 4.5 Å. It is peaked in the center and has broad wings. A maxwellian profile with several keV energy can be fit to the data. However, this is not reasonable, given the presence of a large deuterium flux in the neutral beams, which are at angles close to 90° to the line of sight of the spectrometer. A more subtle analysis is necessary, as follows.

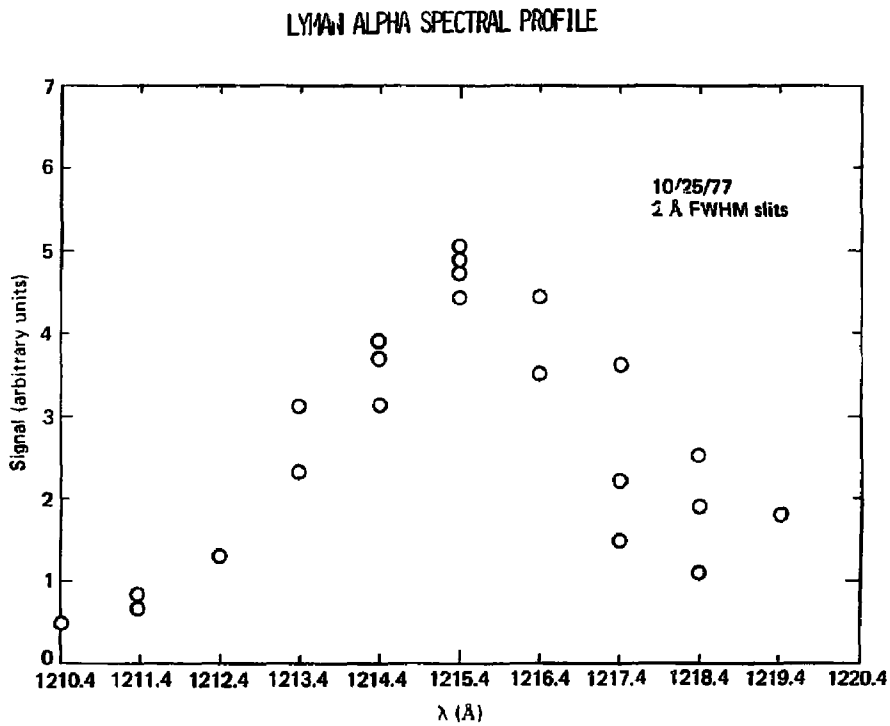

Figure VII-1. The observed spectral profile of Lyman alpha. Each data point is from a single shot.

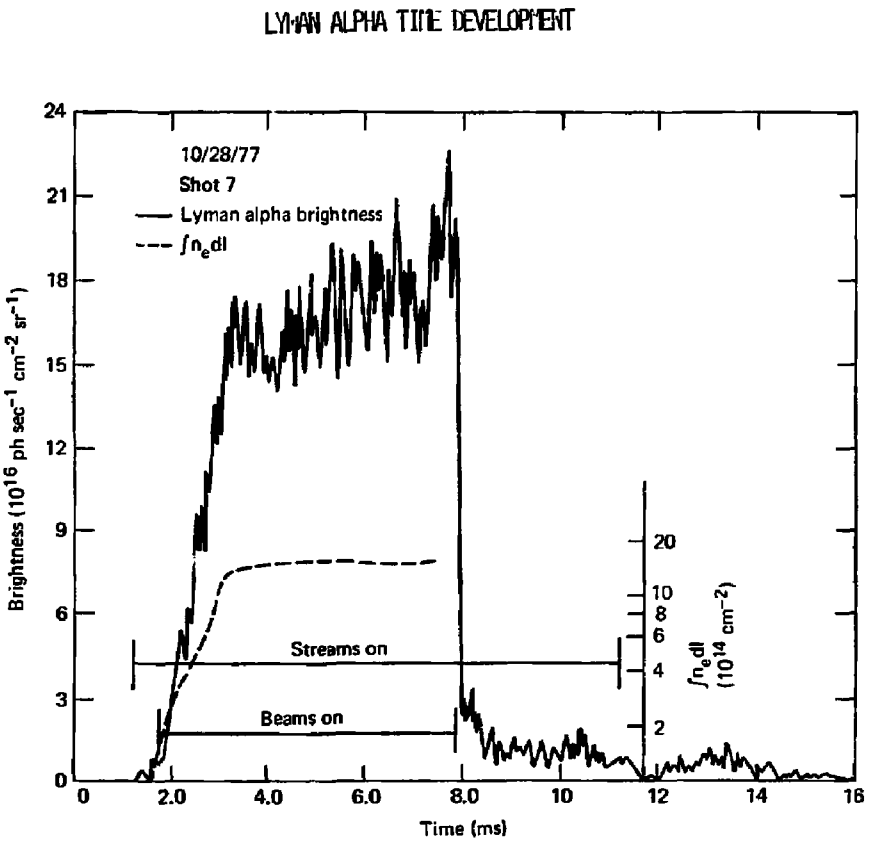

Figure VII-2. The Lyman alpha time development. Wide slits include the entire line.

The neutral deuterium in 2XIIB can be divided into three groups. There is a large charge exchange flux leaving the plasma, which is azimuthally symmetric. This flux results in a broad flat line profile (because of the quite non-maxwellian 2XIIB velocity distribution), with an 8 A FWHM. Secondly, there is a small cold gas flux to the surface of the plasma, producing a triangular profile at the peak of the line. Finally, the untrapped neutral beam particles produce an uneven and possible hollow profile, which is about 4.4 A FWHM, because the beam aiming is not quite perpendicular ($\sim \pm 22^0$) to the spectrometer. Table VII-1 summarizes the Lyman alpha analysis, indicating the brightnesses of the various components of the line, as shown in Fig. VII-3. One concludes that these Lyman alpha observations are consistent with other knowledge of 2XIIB.

Data from the center of the Lyman alpha profile suggests a cold gas brightness of about 1×10^{16}, as this signal remains after the beams have been turned off, eliminating the high energy neutral sources. Modifying Eq. II-(13) for the flux impinging on a plasma surface to include charge exchange,

$$\Gamma = \frac{2\pi B(\langle \sigma v \rangle^{ion} + \langle \sigma v \rangle^{cx})}{\langle \sigma v \rangle^{ex}} \quad .$$

For this brightness, $\Gamma \sim 2.4 \times 10^{17}$ $cm^{-2}sec^{-1}$. Assuming a 27 cm long 8 cm radius plasma, the cold neutral current is about 3×10^{20} sec^{-1}, or about 50 amps at 8 ms.

If this cold neutral current is charge-exchanging on hot plasma ions, the power loss by this mechanism must be large. Such power loss could be as high as 50 amps of 10 keV ions, or 0.5 MW, which is one third the power input to 2XIIB. In that event, the 2XIIB plasma might not sustain itself. One concludes that these measurements are consistent with the existence of a

Table VII-1

LYMAN ALPHA STUDY

Measured Quantities	
Total Brightness	1.7×10^{17} ph/sec/cm^2/ster
Line Center Brightness (2 Å FWHM Slits)	5×10^{16}
Line Width (FWHM)	4.5 Å
Analysis of Components	
Charge Exchange Neutral Profile	
Total Brightness	5.6×10^{16}
Central Brightness	1.3×10^{16}
FWHM	8 Å
Untrapped Neutral Beam Profile	
Total Brightness	1×10^{17}
Central Brightness	2.7×10^{16}
Width	4 Å
Cold Gas Sheath	
Total Brightness	1×10^{16}
FWHM	Thermal

Table showing analysis of lyman alpha profile. Central brightness and all data were taken with a 2 Å FWHM instrument transmission.

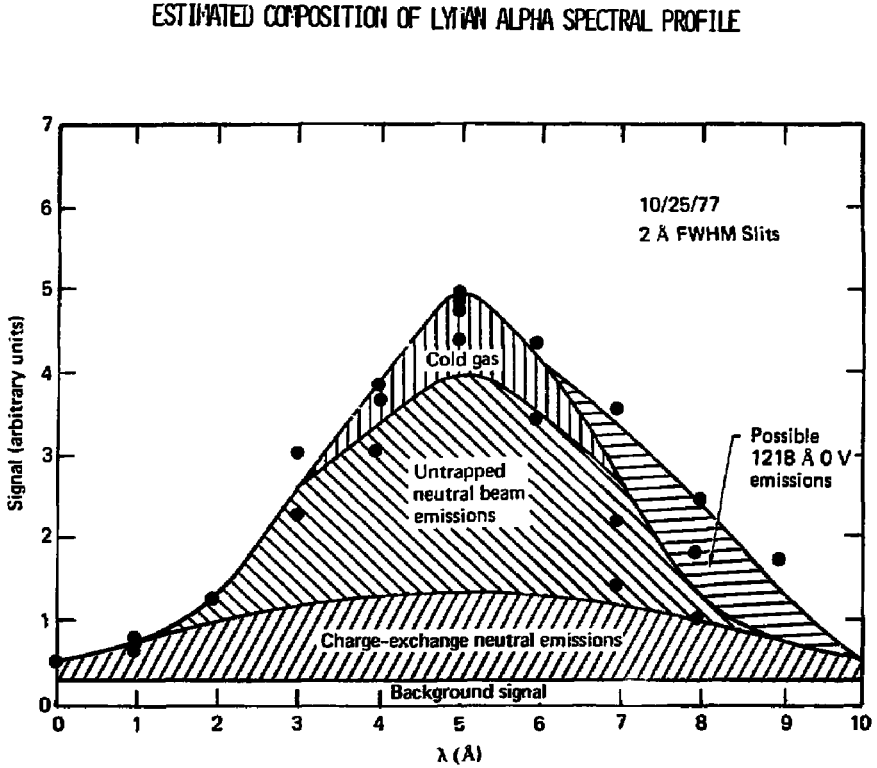

Figure VII-3. The observed spectral profile of Lyman alpha, with estimates of the contributions from various sources.

shielding mechanism,[25] which may consist of accumulated cold gas ions or of plasma ions which diffuse more slowly than they cool.

The Lyman alpha profile is observed to be asymmetric. Examination of the data reveals characteristics in the time dependence on the red side of the line which match those of OV 630 Å. It is speculated on this basis that the OV 1218.4 Å line, a spin-forbidden intercombination transition, may interfere with the 1218 Å Lyman alpha signal. This would be correct if the 1218 Å line were about 10^{-2} times as bright as the 630 Å line.

VIII. CONCLUSION

The major results of this study of 2XIIB are the determination of the principal impurity species and the measurement of the large brightnesses of their EUV emissions. Estimates of impurity power loss, confinement times, and concentrations were also obtained. Table VIII-1 summarizes these results. These measurements have shown that while 2XIIB has impurity radiation density much larger than that of typical tokamaks, the relative power loss due to impurities in the central 2XIIB plasma is comparable to or less than that of the cleanest tokamaks.

The Lyman alpha study was consistent with other knowledge of the 2XIIB plasma. A large cold neutral flux is indicated; this is consistent with the hypothesis of a shielding mechanism protecting the 2XIIB hot ions from charge-exchange on cold gas.

The oxygen confinement time was estimated from the data to be longer than the ejection time for cold impurities affected by the ambipolar potential. This may be because the oxygen is beam injected, or because it is otherwise heated and confined. This and other issues are being investigated in the continuing EUV study of the 2XIIB plasma.

Table VIII-1

Summary of 2XIIB EUV Results

Impurities Identified	Oxygen, Nitrogen, Carbon Titanium
Central Plasma Light Impurities: Density	3%
Power Loss*	60 kW (4% of input)
O VI 1032 Å Brightness	2×10^{18} ph sec^{-1} cm^{-2} sr^{-1}
Z_{eff}	1.9
Dominant Impurity	Oxygen (2%)
Lyman Alpha Brightness	1.5×10^{17} ph sec^{-1} cm^{-2} sr^{-1}
Cold Neutral Current	50 amps at 8 ms

*Radiation from the end fan regions is not included.

ACKNOWLEDGEMENTS

This work was supported by the U.S. Department of Energy through contracts W-7405-ENG-48 at the Lawrence Livermore Laboratory and EY76-S-02-2711 at the Johns Hopkins University.

The authors wish to acknowledge the assistance of the scientific and technical staff of 2XIIB; neither this data nor our understanding of it would have existed without their help.

References

1. Coensgen et al., Phys. Rev. Let. 35, 22, 1501 (1976).
2. Ohkawa, Nucl. Fus. 10, 185 (1970).
3. Magee et al., LASL Report LA-6691-MS.
4. Mattioli, EUR-CEA-FC-761 (1975).
5. Davis, JQSRT 14, 549 (1974).
6. Davis et al., JQSRT 15, 1145 (1975).
7. Davis, NRL Report #33.
8. Lotz, Astroph. J., Supplement 128, Vol. 14, May 1967, pp. 207-238.
9. Gardner, L.D., Ph,. D. Thesis, Yale University, 1978.
10. Crandall, D.H., private communication.
11. Barnett et al., ORNL Report 5206, Vol. 1.
12. Spitzer, Physics of Fully Ionized Gases, Second edition, Wiley, 1962.
13. Futch et al., Plasma Physics 14, 211 (1972) Eq. (44).
14. Equipe TFR, Nucl. Fus. 15, 1053 (1975).
15. Terry et al., JHU Technical Report coo-2711-3 (1977).
16. Coensgen et al., LLL Internal Report UCID-17037 (1976).
17. Soloman and Ederer, Appl. Opt. 14, 1029 (1975).
18. Terry et al., Nucl. Fus. 18, 485 (1978).
19. Simonen et al, Nucl. Fus. 15, 813 (1975).
20. Terry, J.L., Ph. D. Thesis, Johns Hopkins University, 1978.
21. Elton, Atomic Processes, in Methods of Experimental Physics, Vol. 9-Part A, ed. by Griem and Lovberg.
22. Weise et al., NBS report NSRDS-NBS 4, Vol. 1.
23. Terry, J.L. private communication.
24. Coensgen et al., LLL-Prop-148.
25. Stallard et al., LLL preprint UCRL-78741.